Chapter 5

Analysis of Metal-Clad Waveguide

5.1 Introduction

Metal-clad slab waveguides are of interest in the technology of integrated optics. Metallic layers have been made necessary by a number of applications such as connecting the optical components to other circuits, protecting the optical devices against stray light, and heat sinking. Because of their discrimination against TM modes, metal-clad waveguides have also found application in mode and polarization filtering. The characteristics of the waveguides are strongly influenced by the properties of the metals.

Polarization filters are important elements of integrated optical circuits with applications in the processing of signals from optical fiber sensors and in fiber optic gyroscopes. TE mode transmission has been based on the discriminatory absorption of TE and TM modes such as in metal-clad waveguides, [4, 6]. Experimental work

related to TE-pass polarizers has been reported in references [18], [70] and [71]. TM-pass waveguide polarizers have also been reported. These are based on the discriminatory radiation of the TE and TM modes [72, 73].

The basic three layer metal-clad waveguides are characterized by TM waves with much higher absorption loss than TE waves. The use of a low-index buffer layer of suitable thickness between the core and the metallic layer can further enhance the attenuation of TM waves with respect to TE waves [6]. To reverse this effect and realize a TM-pass polarizer a groove adjacent to a channel waveguide has been made with a low-index buffer layer and a metallic layer deposited on the vertical wall of the groove [71]. This approach can be used to fabricate TM-Pass polarizers on already existing waveguides, but it is somewhat elaborate and would require specialized techniques. The method of reference [72] relies on the fact that by coating a waveguide which is just above cut off with a very thin metallic layer, the TE_0 mode becomes cut off while the TM_0 mode remains guided. This approach cannot be implemented in single mode waveguides in which the TE_0 mode is well guided.

TM_o mode transmission can also be obtained in planar metal-clad waveguides when a high-index buffer layer of suitable thickness is introduced between the core and the metallic layer [22]. The waveguide geometry is shown in Figure 1.3.

5.2 Analysis of Metal-Clad Waveguide by MOL

In this section, the Method of Lines (MOL) is applied to analyze the three-layer metal-clad waveguide without a buffer layer (see figure 5.1) and the four-layer metal-clad waveguide with a high-index buffer layer (see figure 5.2) taken from reference [22], the results are compared with published as well as exact results. A close agreement is found between the MOL calculation of the effective indices (real and imaginary parts) and the modal fields with those available in the literature. Gold is used as a cladding to the waveguides. The operating wavelength is chosen to be $1.55\mu m$. Gold has refractive index of $n = 0.1804 + j10.2$ at $\lambda = 1.55\mu m$. The real part of refractive index square ($n^2 = -104 + j3.68$) is negative. A non-uniform mesh scheme is used in the MOL to model the device effectively. There is no need for the absorbing boundary condition (i-e. PML layer) on the metal-clad side of the waveguide, because the metallic cladding absorbs the field.

The calculations are done using the 7-point formulation to efficiently analyze the metal-clad waveguide using the MOL. The number of sample points used in the middle layer (core) is 40 with a total number of 135 sample points used in the entire problem space. For the metal and the buffer layers very fine mesh size (approximately 0.02 micron) is used. The resulting error in n_{eff} (MOL vs. Exact) is 5.72e-8-j3.63e-9. The time required to calculate n_{eff} and the modal field is around 5 seconds (using an IBM Pentium-III machine at 500 MHz with 128 MB RAM running MATLAB 5.2 under Windows 98).

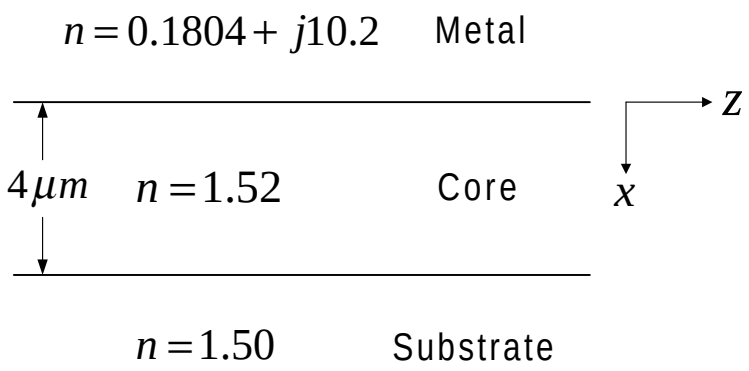

Figure 5.1: Metal-Clad Waveguide without a Buffer Layer

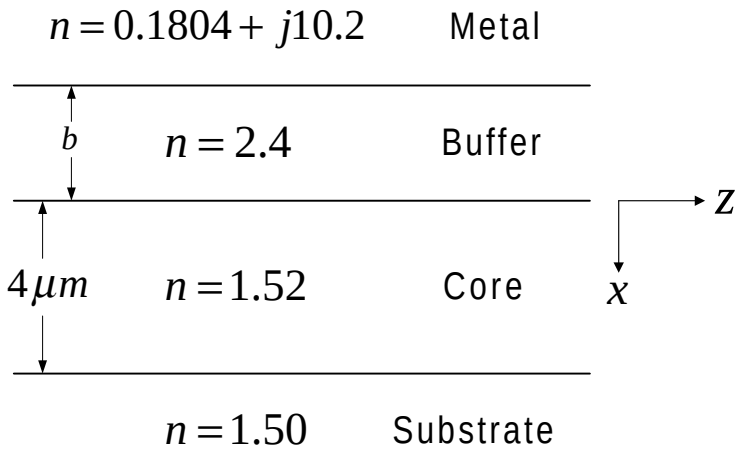

Figure 5.2: Metal-Clad Waveguide with a High-Index Buffer Layer

5.3 Effect of the High-Index Buffer Layer

The metal-clad waveguides shown in figures 5.1 and 5.2 are analyzed by the MOL. The waveguide modes are lossy and therefore have complex effective indices ($n_{eff} = {n_{eff}}' + j{n_{eff}}''$), where ${n_{eff}}'$ is the real part of effective index and ${n_{eff}}''$ is the imaginary part. For guided modes, the real part of the effective index, ${n_{eff}}'$, lies between that of the substrate layer refractive index and the core layer refractive index, that is $1.50 < {n_{eff}}' < 1.52$. The imaginary part of the effective index, ${n_{eff}}''$, is converted into power loss per unit distance, that is in terms of dB/cm. The field patterns of the supported TE and TM modes for both types of waveguides without and with a buffer layer are shown in figures 5.3 and 5.4 respectively. The real and imaginary parts of the effective index and power loss are shown in tables 5.1, 5.2, 5.3 and 5.4.

Without a buffer layer, the TM_0 mode is seen to have higher attenuation (i-e. higher power loss) than the TE_0 mode, while the TE_1 mode is cut-off. This makes the three-layer metal-clad waveguide a TE-pass polarizer.

Mode	${n_{eff}}'$	${n_{eff}}''$	Power Loss (dB/cm)
TE_0	1.51241	2.37701e-6	0.837
TM_0	1.50818	144.93140e-6	51.030

Table 5.1: ${n_{eff}}'$, ${n_{eff}}''$ and Power Loss of the supported TE and TM modes for a Metal-Clad Waveguide without a Buffer Layer at $\lambda = 1.55\mu$m

However, the introduction of a high-index buffer layer of suitable thickness between the core and the metallic cladding enhances the attenuation of all TE modes

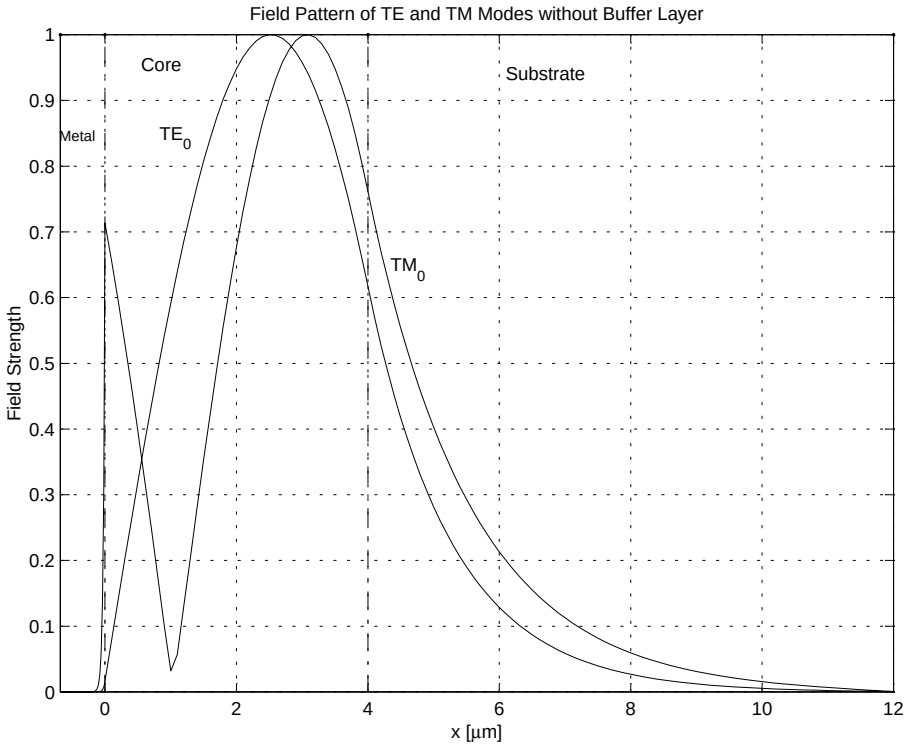

Figure 5.3: Field Pattern for TE and TM modes without a Buffer Layer

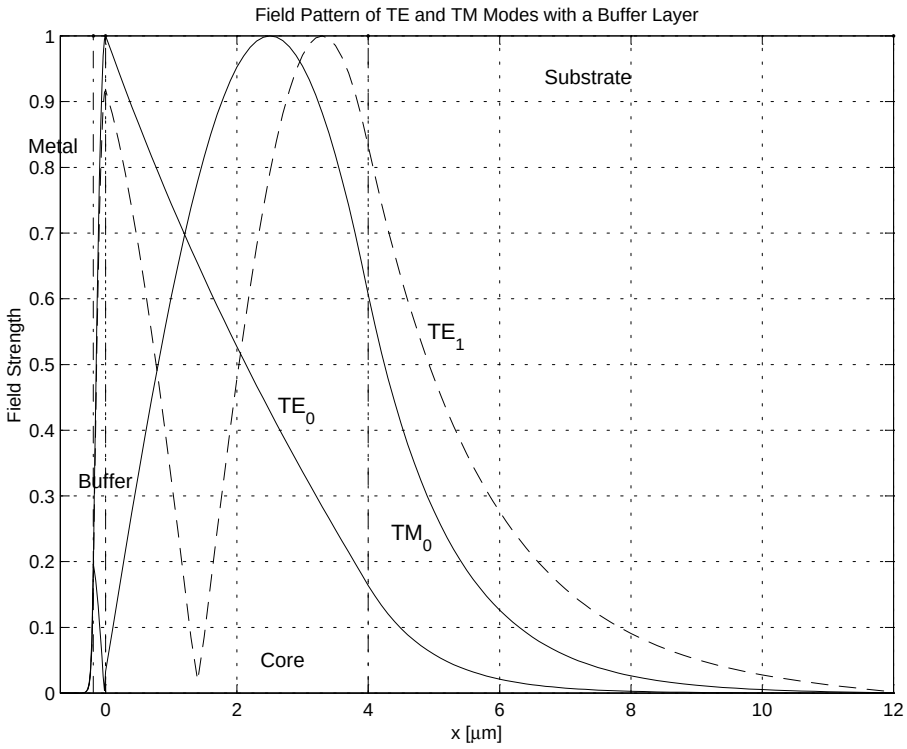

Figure 5.4: Field Pattern for TE and TM modes with a Buffer Layer ($b = 0.190\mu$m)

and reduces the attenuation of the TM_0 mode. This makes the metal-clad waveguide with a high-index buffer layer of suitable thickness effectively a single-mode waveguide and a TM-pass polarizer. Both TE_0 and TE_1 modes decay significantly within a short propagation distance due to their high attenuation constant.

Mode	$n_{eff}{}'$	$n_{eff}{}''$	Power Loss (dB/cm)
TE_0	1.51642	104.28290e-6	36.718
TE_1	1.50261	126.96875e-6	44.705
TM_0	1.51235	4.86571e-6	1.713

Table 5.2: $n_{eff}{}'$, $n_{eff}{}''$ and Power Loss of the supported TE and TM modes for a Metal-Clad Waveguide with a Buffer Layer ($b = 0.180\mu$m) at $\lambda = 1.55\mu$m

Mode	$n_{eff}{}'$	$n_{eff}{}''$	Power Loss (dB/cm)
TE_0	1.51812	177.21914e-6	62.398
TE_1	1.50433	147.99852e-6	52.110
TM_0	1.51239	4.86065e-6	1.711

Table 5.3: $n_{eff}{}'$, $n_{eff}{}''$ and Power Loss of the supported TE and TM modes for a Metal-Clad Waveguide with a Buffer Layer ($b = 0.185\mu$m) at $\lambda = 1.55\mu$m

Mode	$n_{eff}{}'$	$n_{eff}{}''$	Power Loss (dB/cm)
TE_0	1.52102	295.74970e-6	104.133
TE_1	1.50616	141.13064e-6	49.692
TM_0	1.51243	4.88117e-6	1.719

Table 5.4: $n_{eff}{}'$, $n_{eff}{}''$ and Power Loss of the supported TE and TM modes for a Metal-Clad Waveguide with a Buffer Layer ($b = 0.190\mu$m) at $\lambda = 1.55\mu$m

In this case, it is apparent that the introduction of a suitable high-index buffer layer between the core and the metallic cladding converts this waveguide from a TE-pass to a TM-pass polarizer.

5.4 Effect of Varying the Buffer Layer Thickness

We are interested in finding a suitable buffer layer thickness which maximize the power loss of the TE modes and that minimizes the power loss of the TM_0 mode. The mode index or effective index, n_{eff}, is given by $\beta = k_o n_{eff}$. Due to the complex nature of the dielectric constant of the metallic layer all effective indices become complex and are written as $\beta = \beta' + j\beta'' = k_o(n_{eff}{}' + jn_{eff}{}'')$, where $\beta'' = k_o n_{eff}{}''$ is the mode attenuation constant which accounts for the absorption loss due to the presence of the metal.

In figure 5.5 the TE/TM modal loss versus buffer layer thickness (b) is shown. For b=0 the TM_0 mode is seen to have higher attenuation than the TE_0 mode. However, as b increases, the TM_0 mode attenuation begins to decrease while the TE_0 mode attenuation starts to increase and the TE_1 mode becomes guided beyond some higher value of b (b=0.167 μm). For higher values of b, the TE_0 mode attenuation increases while the TE_1 mode attenuation decreases. Buffer layer thickness in the range b=0.17 μm to b=0.20 μm is favorable so that this waveguide functions as a TM-pass polarizer.

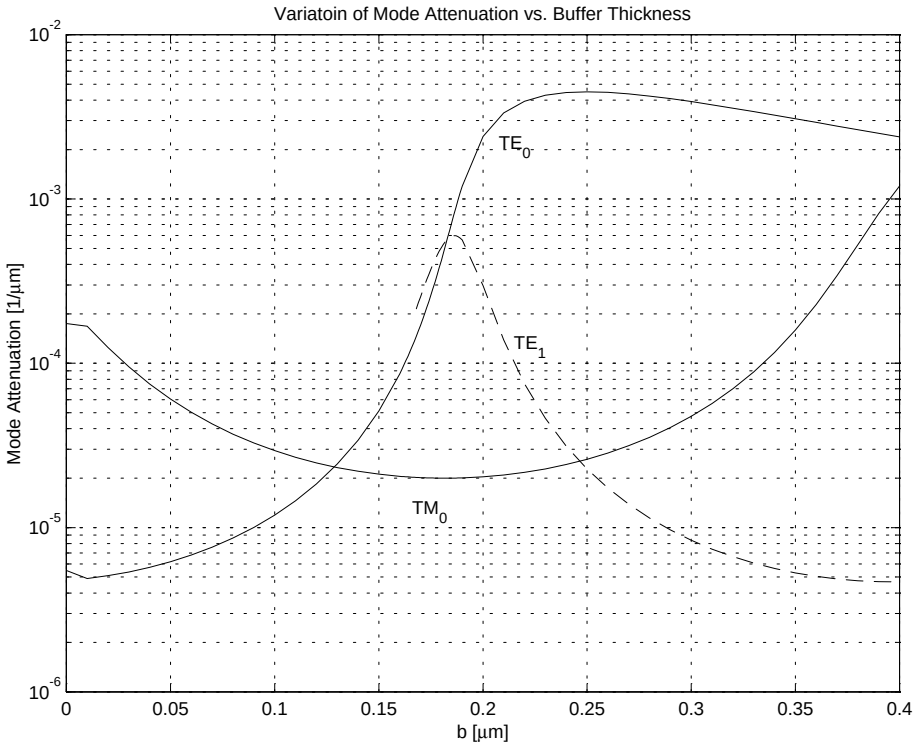

Figure 5.5: Variation of Mode Attenuation (β'') vs. Buffer Layer Thickness (b)

5.5 Comparison of the Exact and the MOL Results

The structure of the TM-pass transmission mode polarizer is shown in figure 5.6. The metal used is Gold which has a refractive index of $n = 0.1804 + j10.2$ at the operating wavelength $\lambda = 1.55\mu m$. A non-uniform mesh scheme is used in the MOL. The PML layer is used as an absorbing boundary condition to absorb the radiation from the two discontinuities at the input and output of the polarizer. A single layer PML is used on top of the computational window and a double layer PML is used at the bottom of the computational window. The first PML layer at the substrate

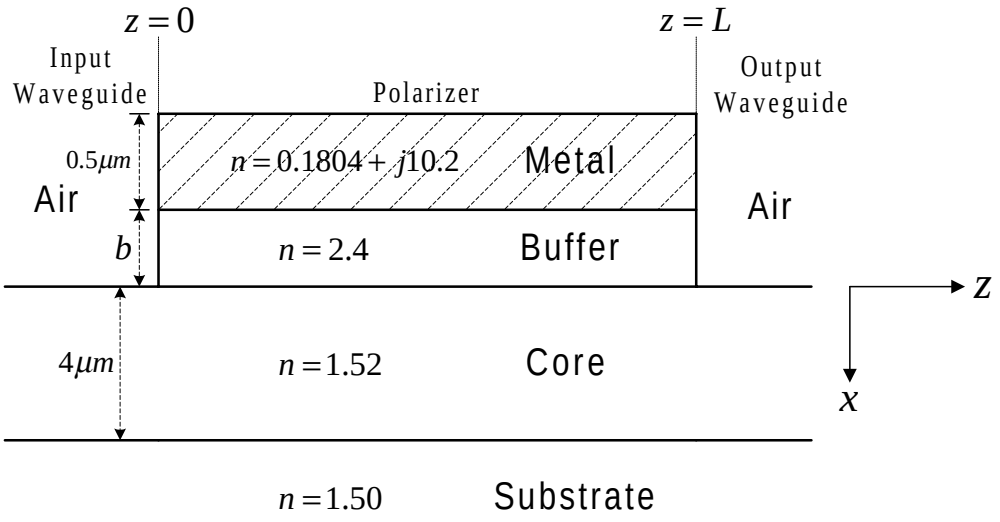

Figure 5.6: TM-Pass Transmission Mode Polarizer

has lower decay factor constant (σ) than the second layer to effectively absorb the radiation at the input and output interfaces of the waveguide. The number of sample points used in each PML layer is 7. The calculations are done using the 7-point formulation. The number of sample points used in the middle layer is 40.

The field patterns of all supported TE and TM modes of the input (and output) waveguide is shown in figure 5.7. The corresponding field pattern of the metal-clad polarizer section is shown in figure 5.8.

To verify the accuracy of the MOL results, the TE_0 and TM_0 mode power loss of the TM-Pass polarizer is plotted against the polarizer length (L) and the results are compared with the exact values obtained by the one-dimensional stationary mode solver program, STF1.

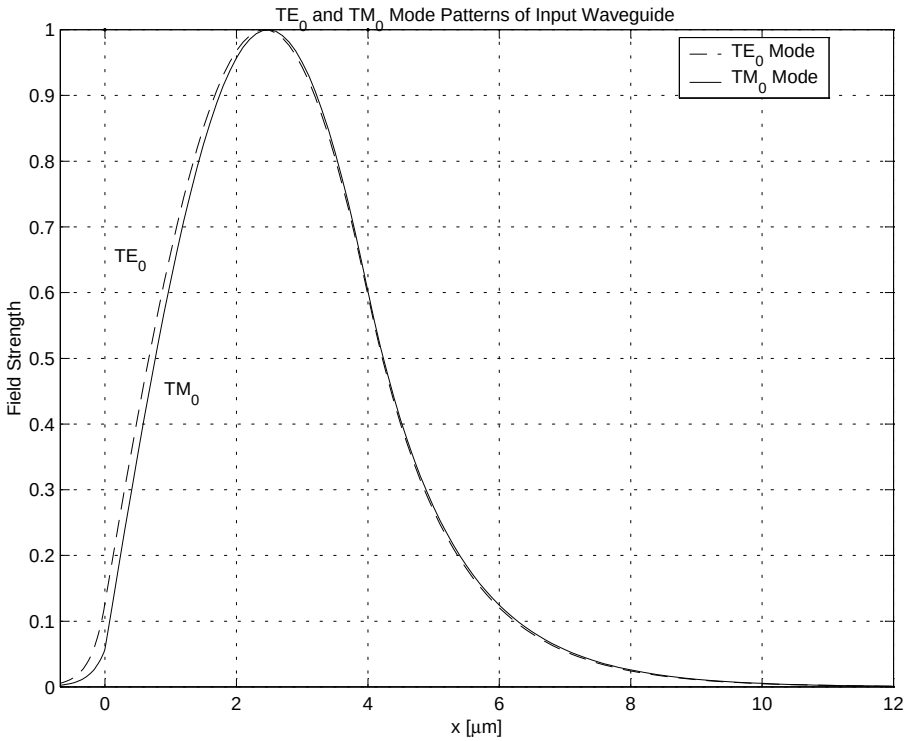

Figure 5.7: TE_0 and TM_0 Mode Patterns of the Input (and Output) Waveguide

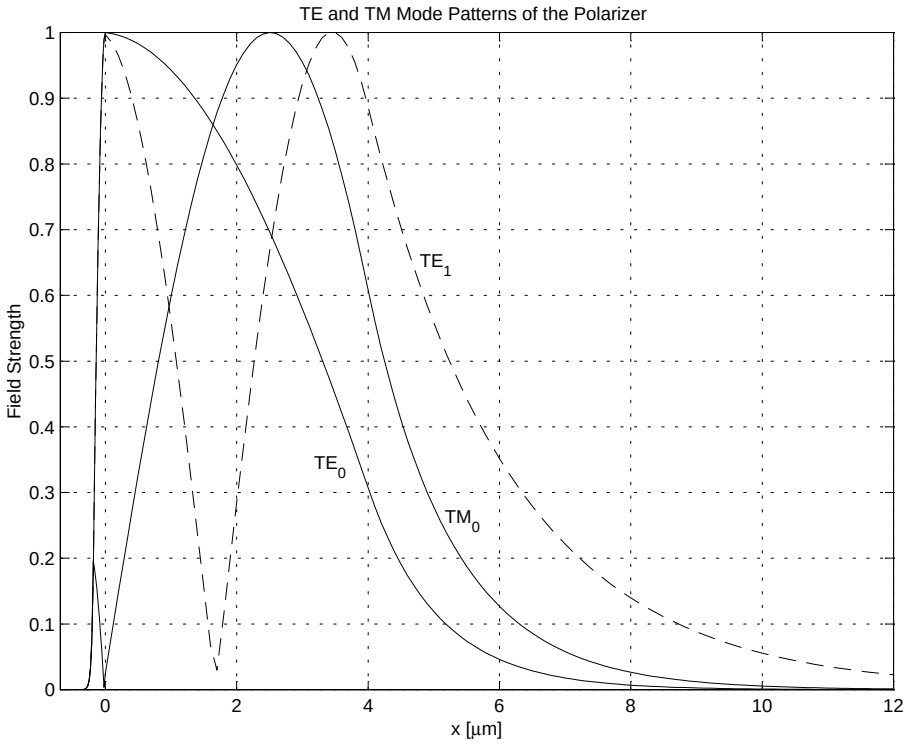

Figure 5.8: TE and TM Mode Patterns of the Polarizer

5.5.1 Calculation of Power Loss by STF1

The STF1 program is written by Al-Jamid. The program listing is shown in Appendix B. This program computes the eigenvalues of guided TE and TM modes of a slab waveguide with an arbitrary number of layers. A zero finding program based on Muller's method [74] is used in conjunction with STF1. The STF1 program gives the exact value of the modal effective index (both real and imaginary parts) and modal field pattern. The imaginary part of the effective index obtained by STF1 is then converted into power loss (dB), using the relation:

$$Power\ Loss = 20\, k_o\, n_{eff}{}''\, L\ log_{10}e \tag{5.1}$$

where L is the length of polarizer.

5.5.2 Calculation of Modal Power and Modal Coefficients in an Arbitrary Field

Any general two-dimensional field $\psi(x,z)$ can be represented as a linear combination of a complete set of orthonormal modes, that is [35]:

$$\begin{aligned}\psi(x,z) &= \alpha_0 f_0(x)e^{j\beta_0 z} + \alpha_1 f_1(x)e^{j\beta_1 z} + \alpha_2 f_2(x)e^{j\beta_2 z} + \cdots + \alpha_m f_m(x)e^{j\beta_m z} + \cdots \\ &\quad + \alpha_M f_M(x)e^{j\beta_M z} + \int_v \alpha_v f_v(x)e^{j\beta_v z}dv \end{aligned} \tag{5.2}$$

where α_m = mth-mode expansion coefficient, β_m = mth-mode propagation constant and $\int_v \alpha_v f_v(x)e^{j\beta_v z}dv$ represents an integration over the continuum of all radiation

modes. The integer M represents the highest possible order of the guided modes. The modal transverse profiles $\{f_m(x)\}$ describe a set of orthonormal functions over the transverse coordinate. For a single-mode waveguide ($M = 0$):

$$\psi(x,z) \;=\; \alpha_0 f_0(x) e^{j\beta_0 z} + \int_v \alpha_v f_v(x) e^{j\beta_v z} dv \tag{5.3}$$

At the input end of the polarizer ($z = 0$) the field ψ becomes:

$$\psi(x,0) \;=\; \alpha_0 f_0(x) + \int_v \alpha_v f_v(x) dv \tag{5.4}$$

By using the orthogonality relation between the modal fields, which is expressed as [75]:

$$\int_{-\infty}^{+\infty} \frac{f_m(x)}{K} f_n(x) dx = \begin{cases} 0 & for\ m \neq n \\ \int_{-\infty}^{+\infty} \frac{f_m^2(x)}{K} dx & for\ m = n \end{cases} \tag{5.5}$$

where K is defined as:

$$K = \begin{cases} n^2(x) & for\ TM\ modes \\ 1 & for\ TE\ modes \end{cases} \tag{5.6}$$

and $n(x)$ represents the refractive index distribution.

The modal coefficient α_m is given by [35]:

$$\alpha_m = \frac{\int_{-\infty}^{+\infty} \psi(x,0) \frac{f_m(x)}{K} dx}{\int_{-\infty}^{+\infty} \frac{f_m^*(x) f_m(x)}{K} dx} \tag{5.7}$$

Hence the coefficient of the fundamental mode α_0 is given by:

$$\alpha_0 = \frac{\int_{-\infty}^{+\infty} \psi(x,0) \frac{f_0(x)}{K} dx}{\int_{-\infty}^{+\infty} \frac{f_0^2(x)}{K} dx} \tag{5.8}$$

The power flowing in the z direction per unit length of the y direction is given by [59]:

$$P_z = \frac{1}{2} \int_{-\infty}^{+\infty} Re(\mathbf{E} \times \mathbf{H}^*)_z dx \tag{5.9}$$

5.5.3 Calculation of Power Loss and Modal Coefficients in the MOL

The field obtained at the output of the polarizer by the MOL is not composed purely of the fundamental mode. This field is a superposition of the fundamental and radiation modes of the output waveguide. Radiation modes decay along the direction of propagation in the waveguide. It is found that these radiation modes are attenuated completely after a propagation distance of $1500\mu m$. Since the input and output waveguides are single-mode the remaining field in the output waveguide after a sufficiently long distance becomes purely composed of the fundamental mode. The fundamental mode power loss can easily be found by squaring the amplitude of the modal field.

In an another method, the overlap integral given by equation 5.8 is used to calculate α_0. In this case we apply equation 5.8 at the input plane of the output waveguide, immediately after the polarizer output.

For TM modes, the incident magnetic field is:

$$H_y = e^{+jS_0 z} A_0 \tag{5.10}$$

where the $M \times 1$ column matrix, A_0, represents the incident field at $z = 0$ and the $M \times M$ matrix $S_0 = \sqrt{Q_0}$ where Q_0 is defined in chapter 3. Using Maxwell's equations, the x component of the incident electric field for TM modes is given by:

$$E_x = \frac{j}{\omega \epsilon_o n_i^2} \frac{\partial H_y}{\partial z} \tag{5.11}$$

where n_i is the sampled refractive index on the ith discretization line. Substituting equation 5.10 into equation 5.11, we have:

$$E_x = \frac{j}{\omega \epsilon_o N} \frac{\partial}{\partial z} (e^{+jS_0 z} A_0) \tag{5.12}$$

$$= -\frac{1}{\omega \epsilon_o N} S_0 e^{+jS_0 z} A_0 \tag{5.13}$$

where the matrix N is defined in chapter 3. Hence, the incident electric and the incident magnetic fields component, E_x and H_y, at $z = 0$ are given by:

$$E_x|_{z=0} = -\frac{1}{\omega \epsilon_o N} S_0 A_0 \tag{5.14}$$

$$H_y|_{z=0} = A_0 \tag{5.15}$$

The average power flow (per unit length in the y-direction) in the z direction is given by:

$$P_z = \frac{1}{2} Re \int_{-\infty}^{\infty} E_x H_y^* dx \tag{5.16}$$

For discrete samples, integration is replaced by summation over the index of the array.

$$P_z = \frac{1}{2} Re \left[\sum_{m=1}^{M} E_{xm} H_{ym}^* \Delta x \right] \tag{5.17}$$

For non-uniform mesh size the Δx can be replaced by $(\Delta x)_m$. Substituting E_x and H_y from equations 5.14 and 5.15 into equation 5.17, we have:

$$P_z = \frac{1}{2\omega\epsilon_o} Re\left[N^{-1} S_0 A_0 A_0^*\right] \Delta x \tag{5.18}$$

Using the modal coefficient formula 5.7, we can calculate the modal expansion coefficient α_m, that is:

$$\alpha_m = \frac{A^t N^{-1} F_m}{F_m^t N^{-1} F_m} \tag{5.19}$$

where the $M \times 1$ vector F_m represents the discretized modal field distribution of the mth mode, A is the discretized general field and the superscript t represents transpose of a vector. The above formula can be used for the TE modes by replacing matrix N with the identity matrix I.

5.5.4 Results

The fundamental mode power loss using the method of lines (MOL) is found by the overlap integral (refer to equation 5.19) and by calculating the fundamental mode amplitude which is obtained after a propagation of sufficiently long distance in the output waveguide. Both methods produce almost identical results and hence, equation 5.19 will be used to find the fundamental amplitude and subsequently the mode power loss throughout in this thesis.

The results by the MOL and STF1 are shown in figures 5.9 and 5.10 for TM_0 and TE_0 modes respectively. For TM_0 mode, the MOL results are in close agreement

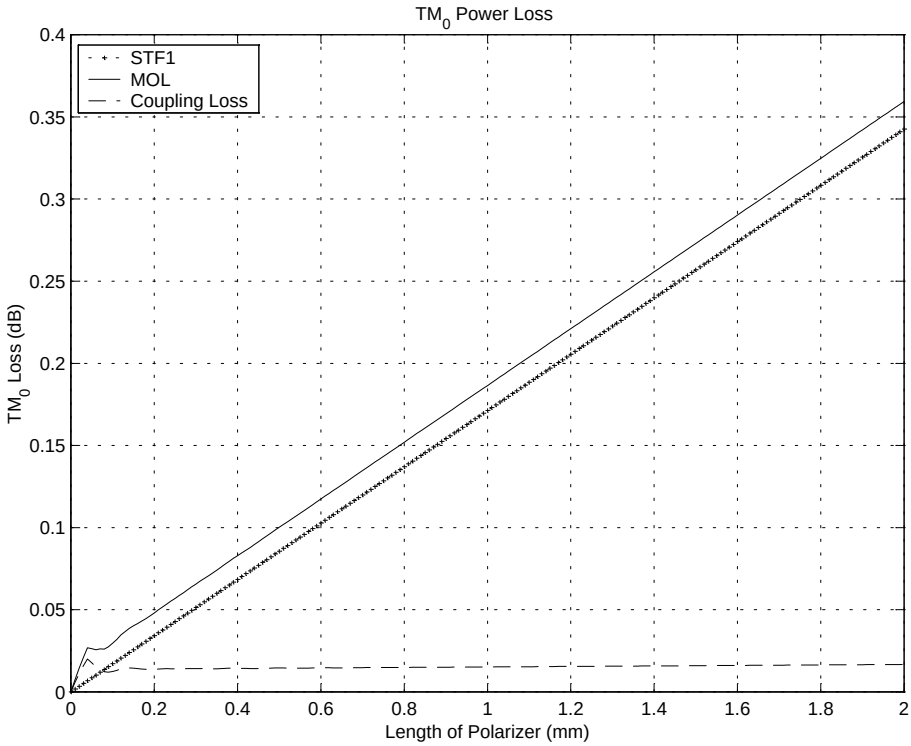

Figure 5.9: TM_0 Mode Power Loss vs. Polarizer Length

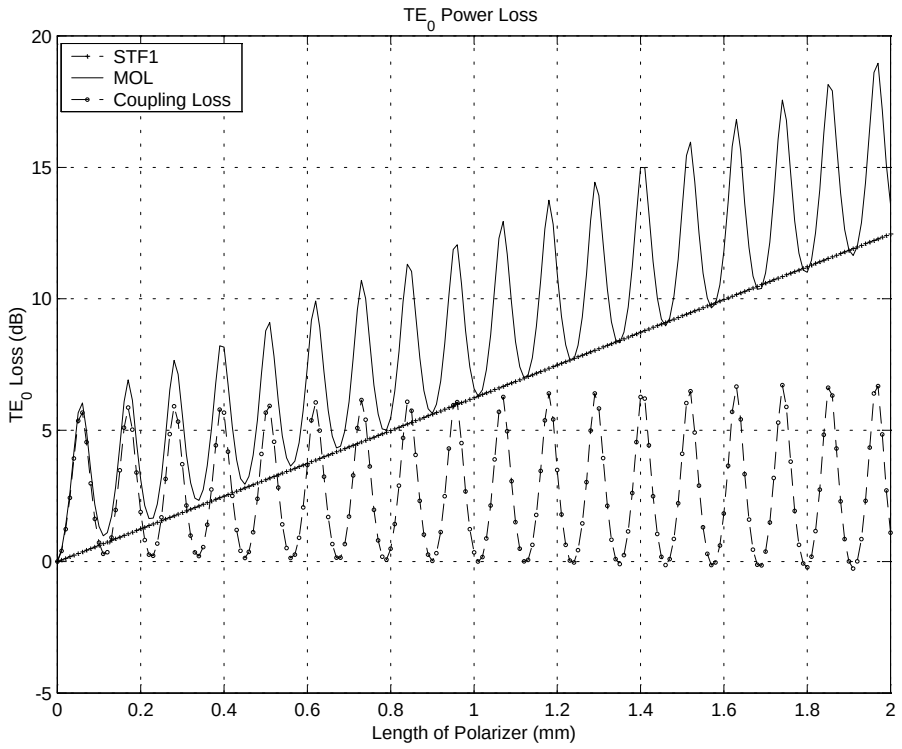

Figure 5.10: TE_0 Mode Power Loss vs. Polarizer Length

with those obtained from the STF1 program. The higher loss of the TM_0 mode as calculated by the MOL is due to the fact that the MOL account for the coupling loss, while STF1 does not. For the TE case, the MOL results are different from the STF1 program. This is due to the interference effect of the TE_0 and TE_1 modes within the polarizer which results in the observed ripples. The absence of these ripples in the STF1 results are due to the fact that STF1 accounts for the fundamental TE mode only and does not account for the interference between the TE_0 and the TE_1 modes.

5.6 Metal-Clad TE-Pass Polarizer

The metal-clad TE-pass polarizer is shown in figure 5.11. The polarizer performance is evaluated using standard methods. The most commonly used performance parameters are the extinction ratio and the insertion loss.

The extinction ratio is defined as the ratio of the power in the desired polarization to that in the orthogonal polarization [71] and insertion loss is defined as the power loss in the desired polarization.

For TE-pass polarizer, the polarization extinction ratio (PER) is given by:

$$PER = 10\ log_{10}\ \left(\frac{Power\ Remaining\ in\ TE_0\ mode}{Power\ Remaining\ in\ TM_0\ mode}\right) \tag{5.20}$$

OR

$$PER = TE_0\ dB\ Loss - TM_0\ dB\ Loss \tag{5.21}$$

where

$$TE_0\ dB\ Loss \;=\; 10\ log_{10}\ (Power\ Remaining\ in\ TE_0\ mode\ at\ the\ output)$$

$$TM_0\ dB\ Loss \;=\; 10\ log_{10}\ (Power\ Remaining\ in\ TM_0\ mode\ at\ the\ output)$$

and polarization insertion loss (PIL) is defined as:

$$PIL = 10\ log_{10}\ (Power\ Remaining\ in\ TE_0\ mode) = TE_0\ dB\ Loss \qquad (5.22)$$

It is assumed that the incident field has unit amplitude and unit power (i-e. 1 Watt), hence the power remaining in a mode is actually the fundamental mode power (i-e. the square of the fundamental amplitude) at the output.

The TE-pass polarizer extinction ratio and insertion loss increase with polarizer length as shown in figures 5.12 and 5.13. The ripples at the beginning of figure 5.12 is due to the interference of the TM_0 and TM_{-1} (surface plasmon) modes. The calculations are done using the MOL with seven-point formulation.

5.7 Metal-Clad TM-Pass Polarizer

The metal-clad TM-pass polarizer (see figure 5.6) performance mainly depends on the buffer layer thickness and polarizer length. The TE_0 loss increases with the polarizer length causing high extinction ratio which is favorable but polarizer insertion loss also increases significantly.

For a TM-pass polarizer, the polarization extinction ratio (PER) is given by:

$$PER = 10\ log_{10}\ \left(\frac{Power\ Remaining\ in\ TM_0\ mode}{Power\ Remaining\ in\ TE_0\ mode}\right) \qquad (5.23)$$

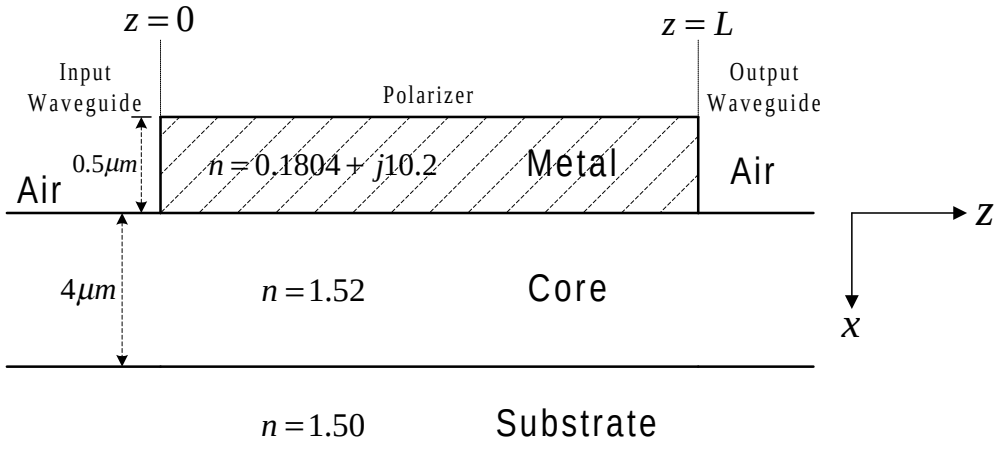

Figure 5.11: Metal-Clad TE-Pass Polarizer

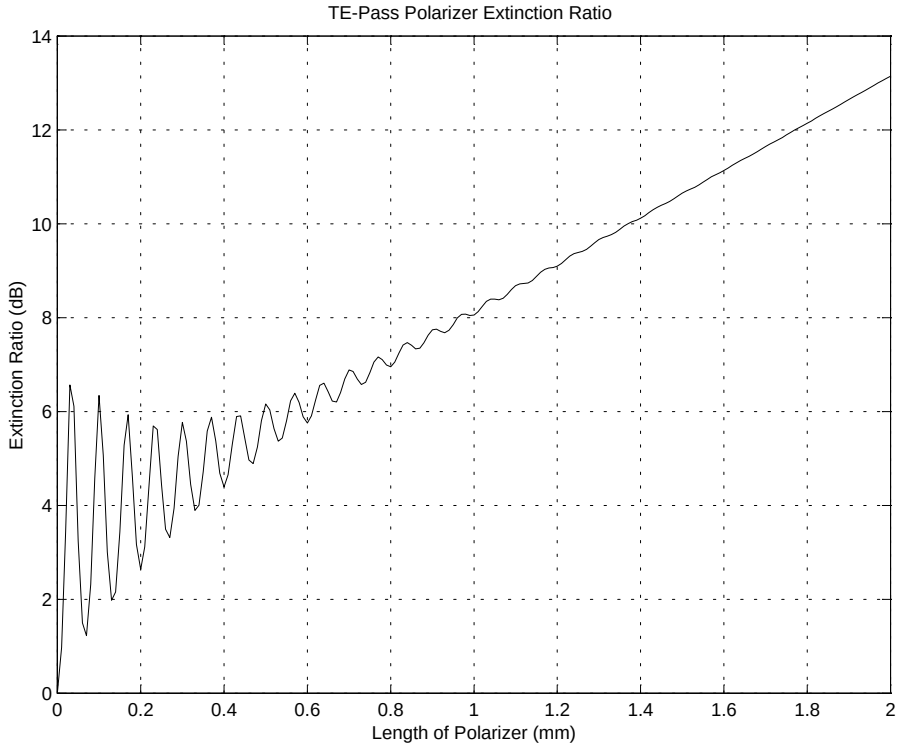

Figure 5.12: TE-Pass Polarizer Extinction Ratio

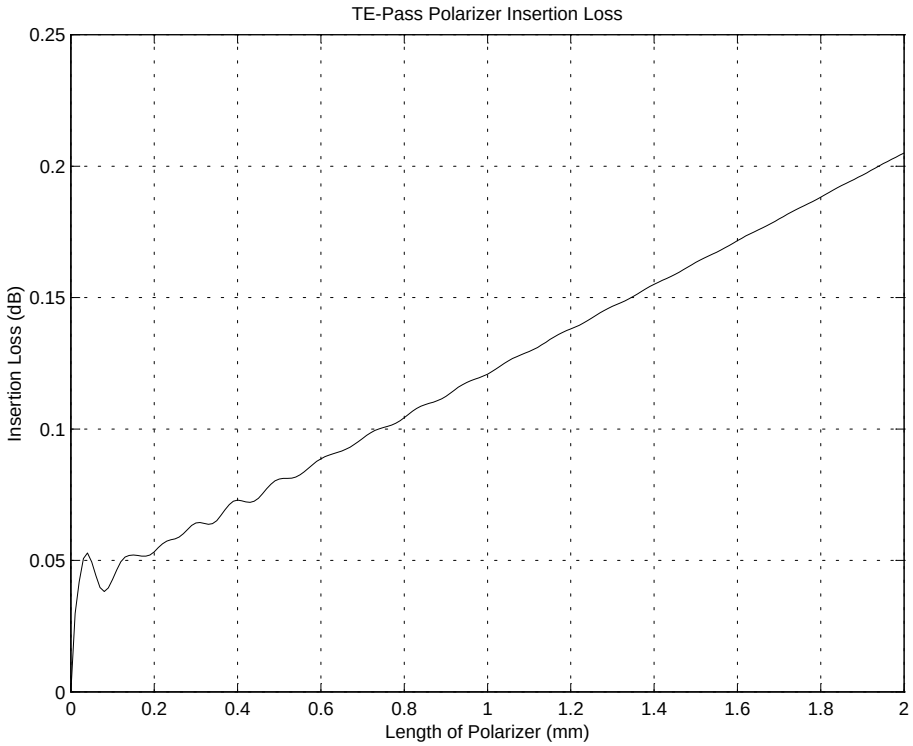

Figure 5.13: TE-Pass Polarizer Insertion Loss

OR

$$PER = TM_0\ dB\ Loss - TE_0\ dB\ Loss \tag{5.24}$$

and polarization insertion loss (PIL) is defined as:

$$PIL = 10\ log_{10}\ (Power\ Remaining\ in\ TM_0\ mode) = TM_0\ dB\ Loss \tag{5.25}$$

The results of the extinction ratio, the insertion loss and the figure of merit for different buffer layer thicknesses are obtained using the MOL with seven-point formulation. It is concluded that the insertion loss has nearly a constant rate of increase for a wide range of buffer layer thicknesses (b=0.175 μm to 0.20 μm) as shown in figure 5.14 while the extinction ratio and the figure of merit are very sensitive to the polarizer length. From figures 5.15 and 5.16, it is obvious that the

extinction ratio is very high for a certain short polarizer length, optimum polarizer length. The extinction ratio at the optimum polarizer lengths for different buffer layer thicknesses is summarized in table 5.5. For simplicity and improved understanding, the extinction ratio with buffer layer thicknesses 0.190 μm and 0.192 μm is shown in separate figures. With buffer layer thickness 0.192 μm and polarizer length 0.05 mm, the extinction ratio is very high as shown in figure 5.16. The short length polarizer offers very low loss in the TM_0 mode case.

Buffer Thickness b (μm)	Optimum Polarizer Length L (mm)	Polarizer Extinction Ratio PER (dB)
0.185	1.97	18.5
0.186	1.95	22.1
0.187	1.93	27.8
0.188	1.47	33.5
0.188	1.58	35.8
0.189	0.91	31.3
0.189	1.23	36.5
0.190	0.47	27.7
0.190	0.68	26.8
0.191	0.15	20.8
0.191	0.56	23.8
0.192	0.05	34.7
0.192	0.15	24.5
0.193	0.05	22.0

Table 5.5: TM-Pass Transmission Mode Polarizer Optimum Lengths for Different Buffer Layer Thicknesses

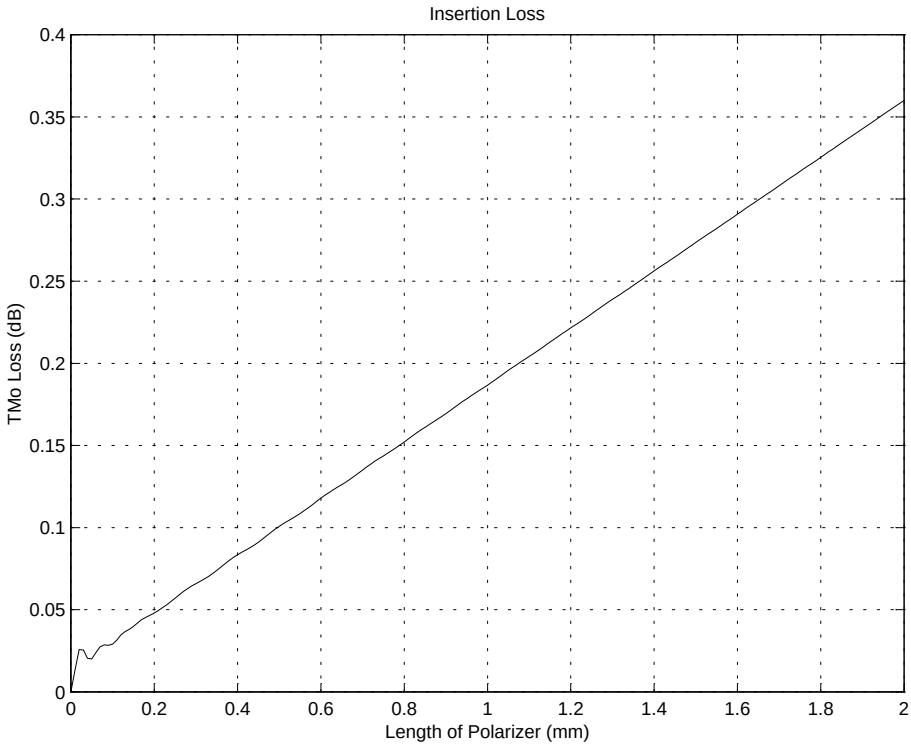

Figure 5.14: TM-Pass Polarizer Insertion Loss

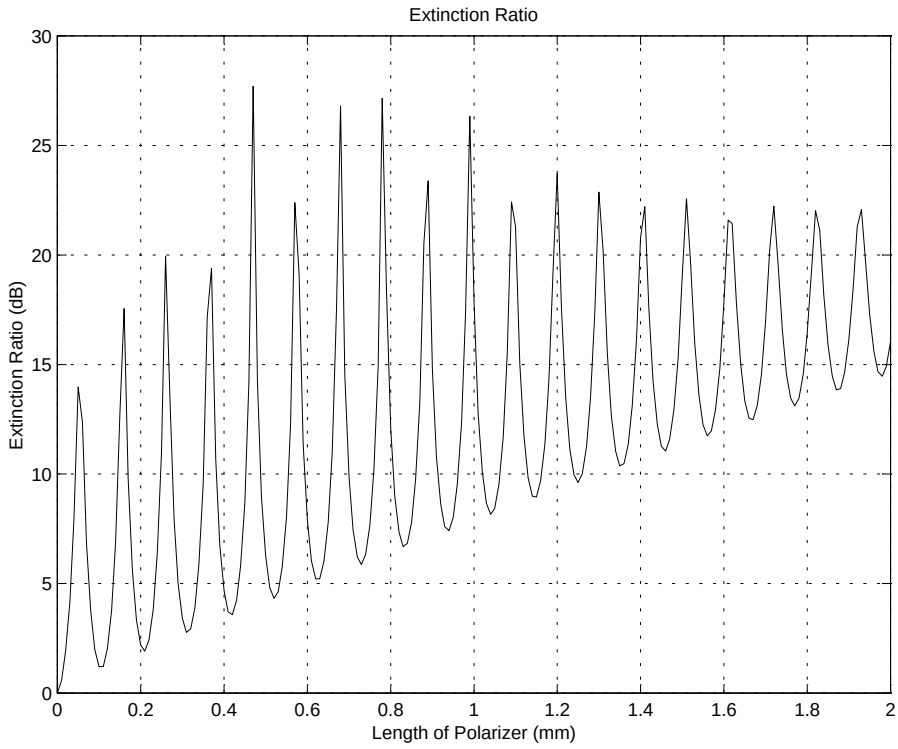

Figure 5.15: TM-Pass Polarizer Extinction Ratio for b=0.190 μm

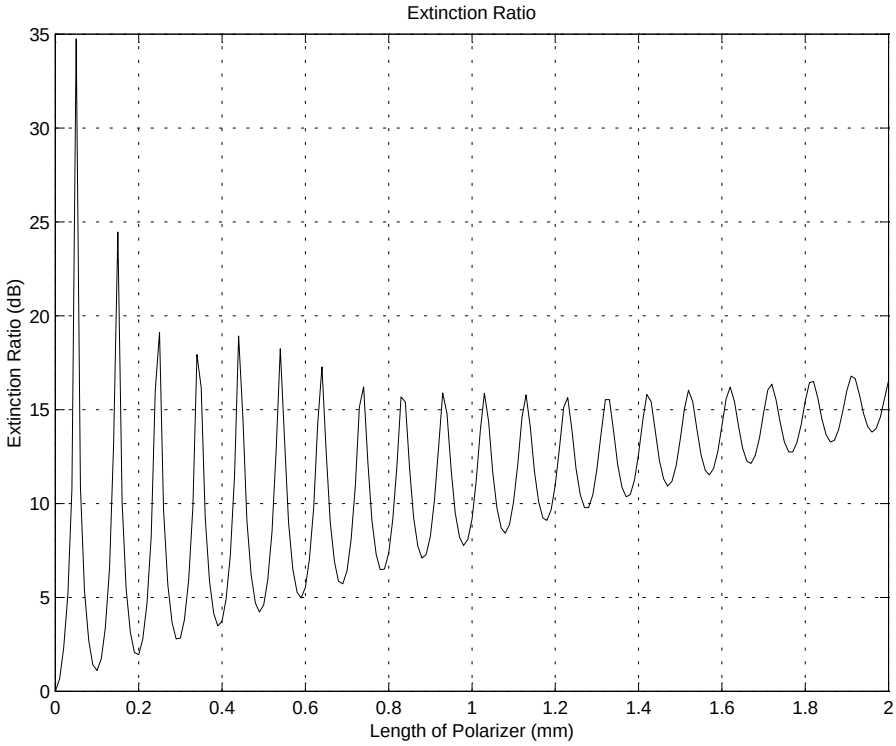

Figure 5.16: TM-Pass Polarizer Extinction Ratio for b=0.192 μm